X-621-68-503
PREPRINT

NASA TM X-63458

A THEORY OF THERMOSPHERIC DYNAMICS PART I: DIURNAL AND SOLAR CYCLE VARIATIONS

H. VOLLAND

DECEMBER 1968

GSFC
GODDARD SPACE FLIGHT CENTER
GREENBELT, MARYLAND

A THEORY OF THERMOSPHERIC DYNAMICS

PART I: DIURNAL AND SOLAR CYCLE VARIATIONS

H. Volland*

December 1968

*NAC/NRC Research Associate, on leave from the Astronomical Institutes of the University of Bonn, Germany.

GODDARD SPACE FLIGHT CENTER
Greenbelt, Maryland

A THEORY OF THERMOSPHERIC DYNAMICS
PART I: DIURNAL AND SOLAR CYCLE VARIATIONS

H. Volland
Goddard Space Flight Center
Greenbelt, Maryland

ABSTRACT

It is shown that the diurnal density and temperature variation within the thermosphere is generated not only by solar EUV heat input but also by a tidal wave from the lower atmosphere which penetrates into the thermosphere and predominates the diurnal variations below 250 km altitude. Assuming a tidal wave from below which is independent of solar activity and assuming solar EUV heat input to be proportional to the solar activity index $F_{10.7}$, the observed diurnal density variation and its dependence on solar activity can be explained and reproduced quantitatively with help of a two dimensional model between 100 and 400 km height. The calculated density agrees with the Jacchia model above 300 km and with observations made by Priester, May, King-Hele, Taeusch and by Marov below 250 km.

A THEORY OF THERMOSPHERIC DYNAMICS

PART I: DIURNAL AND SOLAR CYCLE VARIATIONS

1. INTRODUCTION

Since the launch of the first satellite in 1957, satellite drag measurements and direct in situ observations have rapidly increased our knowledge of the neutral density and its temporal variations within the thermosphere. We can now distinguish basically between the following regular and sporadic density disturbances within the thermosphere (see e.g. the review article by Priester et al., 1967).

Regular effects:

1a. Diurnal variation (Period: 1 day)

1b. Solar rotation variation (Period: 27 days)

1c. Semiannual variation (Period: 0.5 years)

1d. Solar cycle variation (Period: 11 years)

Sporadic effects:

2a. Large scale neutral air waves (Quasiperiod: $\approx$ 1 hour)

2b. Geomagnetic activity effect (Quasiperiod: $\approx$ 1 day)

While the regular disturbances labelled (1) are predictable in occurrence and period, the sporadic effects labelled (2) are not. Nevertheless the last two effects have simple basic features: a train of harmonic waves in case (2a) and an impulse form in case (2b). Thus, they both are accessible to simple model calculations.

Apart from the disturbances mentioned above there exist of course other irregular disturbances without such simple features which we shall not discuss in this paper.

There is general agreement that the effects numbered (1a), (1b) and (1d) are clearly related to solar EUV radiation which is absorbed in the thermosphere and transferred into heat of the neutral air. Effect numbered (2b) is connected with geomagnetic and ionospheric disturbances within the thermosphere and is thought to be caused by solar corpuscular radiation. Effect numbered (1c) is also correlated with geomagnetic activity, but in this case the causal relationship is not known. Effect numbered (2a) which is related to large scale travelling ionospheric disturbances is caused in or below the base of the thermosphere and is interpreted as free internal gravity wave propagation into the thermosphere (Newton et al., 1969). We shall exclude this effect entirely in our subsequent discussions.

The effect, best understood, is the diurnal variation (numbered 1a). The theoretical model of Harris and Priester (1962) connected diurnal EUV heat input with density and temperature variations within the thermosphere. The difficulties of obtaining quantitative agreement between calculated and observed density data in the Harris-Priester model have been settled recently by Volland et al. (1968).

As a working hypothesis Jacchia and other people (see e.g. Priester et al., 1967) invented empirical formulae which relate the exospheric temperature of the static Jacchia model (Jacchia, 1964) or of the Harris-Priester model (CIRA,

1963) to the various activity parameters. This method works well between 200 and 800 km altitude. It fails however to reproduce some observations below 200 km e.g. the semiannual effect and the diurnal variations. Moreover, this method does not provide any insight into the physical processes which cause the various effects.

Some of the problems more or less unsolved until now are the following:

1 At what height is the predominant energy deposited for the various effects and what form and amount of energy is it?

2. What are the reasons for the delay between the time of observed density maximum for the different effects and the assumed time of maximum heating?

We shall try in this paper to give a consistent answer to these questions. Part I deals with diurnal and solar cycle variations. In Part II of this paper we shall treat solar rotation variations, semiannual variations and the geomagnetic activity effect.

2. BASIC THEORY

It has been shown that a two dimensional equatorial model of the thermosphere can explain fairly well basic data of the diurnal tide within the thermosphere between 100 and 400 km altitude (Volland and Mayr, 1968a, Volland et al., 1968). The diurnal variation of density and temperature is generated by solar EUV heat input within the thermosphere and by a tidal gravity wave from the lower atmosphere which penetrates into the thermosphere (see Figure 1). Heat input q, density ρ and temperature T therefore can be separated in the following manner:

$$\left.\begin{matrix} q(x, z, t) \\ \rho(x, z, t) \\ T(x, z, t) \end{matrix}\right\} = c_0(z, t) + c_{EUV}(z, t)\cos\left[\omega(t - \tau_{EUV})\right] + c_{tide}(z, t)\left[\cos\omega(t - \tau_{tide})\right] \tag{1}$$

$$c_0(z, t) + c_{thermo}(z, t)\cos\left[\omega(t - \tau_{thermo})\right]$$

where

$$c_0 \quad \begin{cases} q_0 \\ \rho_0 \\ T_0 \end{cases} \tag{2}$$

are height dependent mean values averaged over one solar day, but slowly varying in time with periods large compared with one day.

$$\Delta c_{EUV} \quad \begin{cases} \Delta q_{EUV} \\ \Delta\rho_{EUV} \\ \Delta T_{EUV} \end{cases} \quad \text{and} \quad \tau_{EUV} \quad \begin{cases} \tau_{q\,EUV} \\ \tau_{\rho\,EUV} \\ \tau_{T\,EUV} \end{cases} \tag{3}$$

are amplitudes and times of maximum of the diurnal disturbance generated within the thermosphere by EUV heat input,

$$\Delta c_{tide} \quad \begin{cases} \Delta q_{tide} \\ \Delta\rho_{tide} \\ \Delta T_{tide} \end{cases} \quad \text{and} \quad \tau_{tide} \quad \begin{cases} \tau_{q\,tide} \\ \tau_{\rho\,tide} \\ \tau_{T\,tide} \end{cases} \tag{4}$$

are amplitudes and times of maximum of the disturbance within the thermosphere generated by the tidal wave from the lower atmosphere. These terms, too, are height dependent and slowly varying with time with periods large compared with one day.

ω is the angular frequency of the earth's rotation,

$\tau = t + \frac{y}{R\omega}$ is the local time,

t is the universal time, y the horizontal distance along the equator, z the height and R the earth's radius.

Δe_{diurn} and τ_{diurn} are amplitudes and times of maximum of the total diurnal disturbance observed within the thermosphere.

The calculations are based on perturbation theory which is a sufficient approximation below 400 km altitude. Since perturbation theory is linear, the variations generated by EUV and by the tidal wave from below within the thermosphere are completely decoupled from each other. Moreover, the physical parameters density and temperature are directly proportional to their respective exciting sources Δq_{EUV} and Δq_{tide}. To obtain agreement between the theoretical results and the observed density, temperature and horizontal wind only the two components of the heat source Δq_{EUV} and Δq_{tide} can be adjusted. These will be chosen so that the density data of Jacchia between 300 and 400 km height and the density data of Priester et al. (1960), May (1963), Marov (1965, 1968), Taeusch et al. (1968) and of King-Hele and Illingston (1967, 1968) below 200 km are reproduced. Then it turns out (Volland and Mayr, 1968a) that the calculated horizontal equatorial wind at 100 km altitude approaches very closely the amplitude

and phase of the diurnal wind derived by Kato (1956) from the geomagnetic S_q current.

We consider only the first harmonics of the diurnal variation, because the diurnal wave is predominant throughout the thermosphere above 150 km altitude. Thus, we can make use of the following relationship that allows a comparison between observations and calculations: If e_{max} and e_{min} are the observed maximum and minimum values of a certain physical parameter during one day then

$$f = \frac{e_{max}}{e_{min}} = \frac{e_0 + e_{diurn}}{e_0 - e_{diurn}} \quad \text{or} \quad \frac{e_{diurn}}{e_0} = \frac{f - 1}{f + 1} \tag{5}$$

is an excellent approximation as long as the diurnal component predominates.

The mean thermospheric density, temperature and molecular weight between 120 and 400 km altitude have been chosen from Jacchia's static diffusion model (Jacchia, 1964) and between 100 and 120 km from CIRA (1965). By this choice we have eliminated the mean heat input q_0.

3. TIDAL WAVE FROM BELOW

A diurnal tidal gravity wave is thermally driven by direct isolation absorption by water vapor in the troposphere and by ozone in the stratosphere and mesosphere (Lindzen, 1967). Its exciting force — solar radiation within the UV and visual light spectrum — does not depend on solar activity. However, its transformation into wave energy and the propagation characteristics of the tidal wave depend on the meteorological conditions which vary with the seasons. We shall show in Part II of this paper that this seasonal variation of the tidal

wave causes the semiannual effect of the thermospheric density. In this paper where we deal only with diurnal and solar cycle variations we consider the tidal wave from below as constant and independent on solar activity.

Since the lower boundary of our model is at 100 km altitudes, and thus far from the height range of the generation of the wave, we must treat the diurnal tidal wave from below as an external energy source (see Figure 1) and consider its magnitude and phase as parameters. In order to adjust this tidal wave to the observed density data of Taeusch et al. (1965) and of King-Hele and Hingston (1967, 1968) as well as to the wind value of Kato (1956) we chose the relative density at 100 km altitude of the tidal gravity wave to be

$$\left.\begin{array}{ll} \dfrac{\rho_{tide}}{\rho_0} & 0.12 \\ \rho_{tide} & 20^{00} \text{ local time} \end{array}\right\} \text{at } z_0 \quad 100 \text{ km} \tag{6}$$

The longitudinal wind component of this tidal wave at the equator at 100 km altitude is then

$$\left.\begin{array}{ll} v_{tide} & 16 \text{ m sec} \\ v_{tide} & 7^{30} \text{ local time} \end{array}\right\} \text{at } z_0 \quad 100 \text{ km} \tag{7}$$

which is close to the value derived by Kato (1956) from the S_q current.

It can be shown that the time averaged vertical energy flux of that tidal wave is of the order of 10^{-2} erg/cm^{2}sec at 100 km altitude. This is two orders of magnitude smaller than Lindzen's (1967) theory predicts. In Lindzen's calculations, dissipation of wave energy due to heat conduction and ion drag has been neglected. Therefore his energy value is probably exaggerated at 100 km altitude. On the other hand, in that height range the diurnal tidal gravity wave belongs to the evanescent modes for which the classical definition of effective vertical energy flux

$$\overline{\Delta E}_{wave} \quad \frac{1}{2} \Delta w \Delta p \cos[\omega(\tau_w - \tau_p)]$$

on which the above mentioned energy data are based is problematic (Volland, 1969). Δw, τ_w and Δp, τ_p are amplitudes and times of maximum of vertical wind and pressure components, respectively, of the wave. Note that for an evanescent free internal gravity wave within an atmosphere of zero heat conductivity we have

$$\omega(\tau_w - \tau_p) \quad \pi/2, \qquad \text{thus} \qquad \overline{\Delta E}_{wave} \quad 0.$$

The tidal wave penetrates into the thermosphere and predominates the horizontal diurnal wind system below 250 km height (Volland and Mayr, 1968a). Most of its wave energy is dissipated by heat conduction and ion-neutral collisions in this height region which heats the thermosphere in addition to the EUV heating. We shall see in Section 8 of this paper that the solar cycle effect provides the possibility of estimating the amount of heat due to the dissipated energy of the tidal wave within the thermosphere.

4. SOLAR EUV HEAT INPUT

Solar EUV radiation is transferred into heat of the neutral gas primarily by photodissociation of O_2 and N_2, by ion recombination and by electron cooling. Photodissociation, the dominant heat mechanism within the lower thermosphere, becomes insignificant at about 100 km and below because at these altitudes almost all of the EUV radiation is attenuated. On the other hand, above 400 km ion cooling is the predominant heat source. However, its heating rate there is at least two orders of magnitude smaller than the heating rate at altitudes between 100 and 150 km. Because of these reasons we confine our thermospheric model to a height range between 100 and 400 km and assume that the variable part of the solar spectrum — namely EUV radiation — is deposited mainly in this altitude range.

The height and time dependence of the various heating mechanisms is not very well known. Harris and Priester (1962) assumed that the heat input is proportional to the ion production rate. Their EUV heating rate for CIRA model 4 ($\overline{F}$ = 125) can be approximated by the following analytical expression

$$\Delta q_{EUV} = 10^{-5} \frac{\Delta E_{EUV}}{H_{EUV}} e^{-(z-z_0)/H_{EUV}} \qquad (8)$$

$$z_{q\,EUV} = 12^{00} \text{ local time}$$

Here, $\hat{}E_{EUV}$ 0.66 erg/(cm^{2}sec) is the diurnal component of the total effective heat input into the thermosphere above 100 km. z_0 100 km is the lower boundary of our model and H_{EUV} 53 km is an empirical scale height.

We shall adopt a heat input of the general form of Equation (8). However, because of our lack of knowledge we consider $\hat{}E_{EUV}$ and H_{EUV} as free parameters in order to adjust our calculations to Jacchia's density data between 300 and 400 km altitude. For simplicity we consider the scale height H_{EUV} as a constant independent on solar activity. The total diurnal EUV heat input is supposed to be directly proportional to the solar activity factor $\bar{F}$ ($\bar{F}$ is the 10.7-cm flux in units of 10^{-22} Watt/m^2 Hz smoothed over two or three solar rotations).

The optimal parameters which for reproducing Jacchia's data in the height range between 300 and 400 km are

$$\hat{}E_{EUV} \quad 0.27 \frac{\bar{F}}{125} \quad \text{erg/(cm}^2\text{sec)}$$
$$H_{EUV} \quad 100 \text{ km} \qquad (9)$$

We shall use these parameters in the following calculations.

Our scale height H_{EUV} is larger by a factor of two than the value derived from Harris and Priester's (1962) calculations. This is not surprising because we shall see in section 6 that the EUV heat input significantly influences the thermospheric density variations only above 250 km altitude. The heating of the thermosphere at these heights is provided mostly by the plasma of the ionosphere. Thus, the height distribution of the heating rate not only depends on the neutral

density but also on the density and temperature distribution of the electrons. Our scale height H_{EUV} approximates the EUV heat distribution between about 300 and 400 km altitude. The real heating rate certainly is much more complex than Equation (8) exhibits.

5. COLLISION NUMBER

Collisions between neutrals and ions play a decisive role in the dynamics of the thermosphere at F2-layer heights. There, collisions between oxygen-atoms and oxygen-ions predominate. Dalgarno (1964) gave the formula for collisions between oxygen-atoms and -ions:

$$\nu_{in} = \nu_{ei} = 10^{-10} N_i \qquad \text{sec}^{-1} \tag{10}$$

where the factor ν_{in}/ν_{ei} varies between 5 and 10 at ion temperatures between T_i = 400° and 2000° K, and N_i (in cm^{-3}) is the number density of O-ions. Near the equator the real height of the F2-layer is between 300 and 400 km. We approximate the time averaged collision number ν by the analytical expression

$$\nu = \frac{1}{3}\left(2 + \frac{\bar{F}}{125}\right)\nu_{max}\, e^{-b(z-z_{max})^2} \tag{11}$$

where $\nu_{max} = 4 \times 10^{-4}$ sec^{-1} is the maximum collision number at the maximum height $z_{max} = 350$ km for $\bar{F} = 125$, and $b = 7 \times 10^{-5}$ km^{-2} determines the height dependence of ν. The bracket on the right side of Equation (11) allows for a variation of ν by a factor of two between solar minimum and solar maximum. According to Equation (10) the value of ν in Equation (11) for $\bar{F}$ = 125

corresponds to an ion density and an electron plasma frequency f_p, respectively, of $N_i \approx 5.5 \times 10^5$ cm^{-3} and $f_p \approx 6.7$ MHz.

Equation (10) is oversimplified at E-layer heights. There, the collision cross section decreases due to the change in the major constituents of plasma and neutral air. However, because of the small ion number density at this height range the influence of ion drag on the diurnal wave becomes small. It can be shown that the exact altitude profile of , determined by the exponential factor b in Equation (11), is not of great significance for the diurnal dynamics. However, the absolute value of maximum collision number ν_{max} within the maximum F2-layer has an important influence on the time response of the thermospheric density with respect to solar EUV heating. This is shown in Figure 2 where the time of maximum τ_{EUV} of the diurnal density variation at 350 km altitude has been calculated for values of ν_{max} varying from 10^{-5} to 10^{-2} sec^{-1}. We note immediately that the observed time delay of 2 hours in the density variation (maximum at 14^{00} local time) with respect to the EUV heat input (maximum at 12^{00} local time) corresponds just to the collision number derived from Equation (10) and from the observed time averaged maximum electron density of the equatorial F2-layer (see upper scale in Figure 2 where the ion number density is scaled).

The observed time lag of two hours of the thermospheric density is therefore the natural time response of the thermosphere to the EUV heat input. The dependence of this response time on the collision number results from the strong influence of on the horizontal winds. The maximum longitudinal wind speed Δv_{EUV} of the diurnal wave at 350 km altitude is plotted versus ν_{max} in Figure 2

as dashed line. The collisions act like a "resistance" within an oscillator system. On the other hand, the horizontal winds determine the convective heat capacity of the thermospheric "condensor". An increase of the collision number leads to a decrease of the horizontal wind speed, thus to an increase of the convective heat capacity and an increase of the time lag. For small horizontal velocities the time lag becomes 3 hours (corresponding to a density maximum at 17^{00} local time). This is just Harris and Priester's (1962) result in their one dimensional vertical model in which horizontal winds have been neglected. A decrease of the collision number gives rise to a phase advance of the density maximum with respect to the EUV heat source which becomes 90° (or 6 hours) at small collision numbers. This is the direct result of the decreasing resistance and of the decreasing convective heat capacity within the thermospheric "circuit system".

The relative amplitude $\Delta\rho_{EUV}/\rho_0$ is not influenced very much by the collision number ν_{max}.

6. DIURNAL AND SOLAR CYCLE VARIATIONS

Using the assumptions about the energy input made in section 2 to 5 and using Jacchia's static diffusion model for the mean values [Jacchia (1964)] our thermospheric model of the diurnal variations over the period of one solar cycle is uniquely determined. Figure 3 shows the relative amplitude of density and temperature variations versus height due to the internal EUV heat input [Equations (8) and (9)] for four different solar activity factors $\bar{F} = 62.5$, 125, 187.5 and 250, equivalent to Jacchia's exospheric temperatures of $T_\infty = 750°$, 1000°, 1250° and 1500°K. Though the heat input increases with increasing $\bar{F}$, the relative amplitudes decrease at altitudes above 200 km. This results from the

fact that mean density ρ_0 and mean temperature T_∞ increase more with F than the diurnal variation. However, the absolute amplitudes ρ_{EUV} and T_{EUV} at 100 km altitude, plotted versus F in Figure 4, increase with F. Below 200 km the strong heat input causes a minor increase of the relative amplitude with increasing solar activity. However, the relative density variation due to EUV is smaller than 2% there and is of no significance.

Figure 5 shows the relative amplitudes of density and temperature for the contributions due to the tidal wave from below. The tidal wave propagates freely through the thermosphere. Between 100 and 400 km altitude about 98% of its wave energy is dissipated by heat conduction and ion drag. Therefore the relative density amplitude remains roughly constant with height while the relative temperature amplitude decreases between 150 and 300 km altitude. The decrease of the relative amplitudes with increasing solar activity is again the result of the strong increase of the mean values with F. In Figure 4 we notice that the absolute density variation generated by the tidal wave increases with F, while the temperature variation remains constant. This results from the changing propagation conditions within the thermosphere with solar activity because according to our assumptions the tidal wave input at 100 km does not depend on solar activity.

The sum of both contributions is plotted in Figure 6 versus height for the four exospheric temperature values T_∞. The dashed lines in Figure 6 are Jacchia's equivalent day to night ratios converted into relative amplitudes by Equation (5). The full and open circles are N_2 measurements by Taeusch et al. (1968) and satellite drag measurements by King-Hele and Hingston (1967, 1968) made at moderate solar activity (F 100 - 150). We repeat that the four

available parameters of the two heat sources in our model have been chosen such that Jacchia's data between 300 and 100 km and Luensch's and King-Hele's data below 200 km at F 125 could be reproduced.

Our results show that in view of our highly idealized model the agreement between Jacchia's density data and our calculations is excellent above 300 km. The dependence of the relative density amplitudes on solar activity is well reproduced. The largest differences appear at highest solar activity. It is of course possible to obtain even better agreement by allowing an increase of the scale height H_{EUV} with solar activity of the EUV heat energy rate in Equation (8).

Below 250 km altitude we notice a strong deviation of our density data from Jacchia's densities. This is due to the fact that Jacchia forced his density variations to become zero at 120 km altitude while in our calculations the tidal wave predominates at this height range. At 200 km altitude Priester et al. (1960) and May (1963) observed relative density variations of 15 in 1958 during higher solar activity while King-Hele and Quinn (1965) and Marov (1965) during low solar activity in 1963 gave day to night ratios of f 1.7 to 1.9. These data are correctly reproduced in our model. Our temperature amplitudes are systematically lower than Jacchia's data above 200 km altitude. The difference increases with increasing solar activity. This discrepancy will be explained in the next section.

Figure 7 gives the time of maximum of density and temperature variations due to the two heat sources versus height for T_∞ 1000 K (F 125). We notice that the EUV contribution (dashed lines) has the time of maximum at 14^{00} local time for density and temperature above 200 km height. The tidal density maximum

varies from 20^{hrs} at 100 km to 11^{hrs} at 100 km altitude while the tidal temperature is at 10^{hrs} at 100 km giving rise to a phase difference of 1 hours with respect to the EUV generated temperature (dash-dotted lines). The time of maximum of the total density variation (full lines) remains within day time above 150 km which is in agreement with observations of Marov (1968), King-Hele and Kingston (1967) and Taeusch et al. (1968). Also the time of maximum total temperature variation which is at 13^{hrs} local time above 150 km occurs at day time in reasonable agreement with observations of Taeusch et al. (1968).

The times of maximum are very insensitive to solar activity and show deviations from the data plotted in Figure 7 which generally are not larger than 30 minutes.

In the whole altitude range above 100 km there is no isopycnic layer where the density variations become zero.

Figure 8 shows the diurnal horizontal and vertical wind speed plotted versus height and calculated for different solar activity factors F. The horizonal wind (positive in the east direction) decreases with increasing solar activity in the entire height range while the vertical wind is not influenced very much by solar activity. The horizontal wind has a relative minimum near 350 km altitude, which results from the maximum ion drag near the F2-layer maximum. The EUV and the tidal contributions of the winds have been plotted in Figure 8 as dashed and as dash-dotted lines respectively only for $\bar{F}$ = 125 ($\bar{T}_\infty$ = 1000 K) in order to show their typical behavior. We notice that the tidal component of the winds predominates below 300 km altitude. The horizontal wind responsible for the S_q current at E-layer heights is entirely due to the tidal wave from below.

In Figure 9 the time of maximum of the different wind components and of the total wind has been plotted versus height for I = 125°. Again this time of maximum is only insignificantly influenced by solar activity.

The squares in Figures 8a and 8a indicate Kato's (1956) wind of the diurnal component of the S_q current at the equator. They fit well with the calculated values.

The horizontal wind strongly depends on the collision number ν. The height profile of ν was given by Equation (11). Therefore we expect a very sensitive reaction of the horizontal wind to changes in the ν-profile. This is in fact the case. For example, the calculations by Volland et al. (1968) were based on a ν-profile which increased exponentially with height. The horizontal wind therefore did not show the relative minimum as Figure 8a indicates. However, the wind speeds are of the same order of magnitude. Also the times of maximum are nearly the same. Moreover, all other parameters like vertical wind, density and temperature are not significantly influenced by that change in the ν-profile. This shows that the horizontal wind essentially exerts only a second order effect on the diurnal variations. Its integral amplitude can shift the phase of the density maximum (see Figure 2) but does not influence very much the amplitude of the density.

7. LIMITATIONS OF THE MODEL

We have seen in Figure 6 that our temperature amplitudes are systematically lower than Jacchia's data above 200 km altitude. The reason for this discrepancy is twofold.

First, agreement between both model temperatures can be expected only if both density profiles are the same. This is not the case during high solar activity and at altitudes below 200 km. Our density scale height is smaller than Jacchia's density scale height for F 250. Therefore our temperature variation must be smaller than Jacchia's values in accordance with the results in Figure 6.

Second, in our calculations we neglected the time variation of molecular weight which is due to changing composition from day to night. The barometric height formula is an excellent approximation even for the diurnal variations. Our temperature values should therefore agree with Jacchia's data if both density profiles are the same. From Figure 3a we notice that both density profiles agree at T_∞ 750 and 1000 above 300 km altitude. Jacchia's temperature gradient is nearly zero above 300 km height. Our temperature gradient is also small and can be taken as zero. Therefore the barometric height formula becomes

$$\frac{1}{\rho}\frac{\partial \rho}{\partial z} \qquad \frac{1}{H} \tag{12}$$

where

$$H \quad \frac{RT}{Mg}$$

is the density scale height assumed to be equal in Jacchia's model and in ours. The diurnal variation of the scale height is then

$$\frac{\Delta H}{H} \quad \left(\frac{\Delta T}{T}\right)_V \quad \left(\frac{\Delta T}{T}\right)_J - \frac{\Delta M}{M} \tag{13}$$

where $(\Delta T/T)_J$ is the relative temperature amplitude of the Jacchia model and $(\Delta T/T)_V$ is our temperature amplitude because we neglected the diurnal variation

of the molecular weight M. The difference between both temperature amplitudes is due to the diurnal change of M. At 100 km altitude and for T_∞ = 1000 K it is according to the Jacchia model

$$\frac{M}{M} = 0.82$$

Therefore

$$\left(\frac{T}{T}\right)_{\max} \Big/ \left(\frac{T}{T}\right)_{\min} \frac{M}{M} = 1.23 \cdot 0.82 = 0.87$$

which is very near to our value calculated in Figure 3b. We should however bear in mind that the absolute error in the temperature amplitude for T_∞ = 1000 K is not larger than 30 K.

The maximum difference between Jacchia's and our temperatures is 90 K at 400 km altitude during maximum solar activity (see Figure 4). In Figure 10, maximum and minimum temperatures at 100 km altitude are plotted versus solar activity factor F together with Jacchia's day and night exospheric temperatures (dashed lines). We notice that the difference between Jacchia's temperatures and ours never exceeds 6% of the total temperature which is certainly within the range of accuracy of any direct temperature observation.

It is possible to remove the error in the temperature variation of our model which is due to the neglect of the temporal composition changes. This can be done by an iteration process. Furthermore, for the expressions of the EUV heating rate [Equation (8)] and of the collision number [Equation (11)] simple analytical functions have been chosen deliberately in order to find out their basic

influence on the diurnal dynamics. Improved and more complete observational data especially in the height range below 300 km will certainly modify the numerical values of these parameters and of the tidal wave input. Our model is flexible enough to allow for such modifications. It is in fact capable of determining the height distribution of the solar EUV heat source and of the collision number if appropriate density and wind data are available. In this connection it is perhaps of interest that the model calculations for the entire solar cycle on which the data plotted in Figures 3 to 10 are based upon have been performed in the time of one minute during a single computer run on the IBM 360/75.

Our two dimensional model of course is not able to explain latitudinal effects. The global behavior of the diurnal dynamics must be treated with help of a three dimensional spherical model (Volland and Mayr, 1968b). That the two dimensional model nevertheless describes rather well the low latitude behavior of the diurnal tidal variations of the thermosphere is due to the fact that the diurnal thermospheric tides are predominated by the spherical function P_{11} which is an eigenfunction of the spherical problem. $P_{11} \sim \sin\theta$ (θ is the co-latitude) varies only slightly with θ at low latitudes and therefore can be treated as a constant there.

A word must be said about the validity of perturbation theory which we used entirely in our calculations. We state that perturbation theory is an excellent approximation as long as the relative amplitudes of the perturbated values do not exceed the number 0.5. This condition is fulfilled in our calculations within the height range between 100 and 400 km for all parameters with the exception of v_{diurn}/v_0 at low solar activity ($\bar{T}_\infty \sim 750°K$; see Figure 6). The error due

to perturbation theory can best be estimated in the equation of state. The relative pressure amplitude is

$$\frac{\Delta p}{p_0} \quad \frac{\Delta \rho}{\rho_0} + \frac{\Delta T}{T_0} = \frac{\Delta M}{M_0} + \frac{\Delta \rho}{\rho_0} \frac{\Delta T}{T_0} \tag{14}$$

Apart from the variation of molecular weight M which we already discussed we neglected the last term on the right side of Equation (14) in our perturbation theory. At moderate solar activity (T_∞ 1000°K) and at 400 km altitude this term has the value (see Figure 6)

$$\frac{\Delta \rho}{\rho_0} \frac{\Delta T}{T_0} \quad 0.5 \times 0.1 \quad 0.05.$$

However, this error of 5% does not appear in the diurnal component but is transferred into the semidiurnal component and into the mean value ρ_0. The semidiurnal component likewise transfers part of its energy content into the diurnal component. As long as the semidiurnal component is small, our perturbation theory is valid within the limits mentioned above. It gives of course only the first harmonic or the diurnal component of the diurnal disturbance. Fortunately the semidiurnal component is in fact small at least above 150 km altitude as the observations confirm. This smallness is caused by the filter action of the thermosphere which suppresses higher harmonics of the propagation modes (Volland, 1969).

8. CONCLUSION

By treating a two dimensional model of the thermosphere at low latitudes it has been shown that the diurnal density disturbance is generated by solar EUV heat input within the thermosphere and by a tidal wave from the lower atmosphere

which penetrates into the thermosphere and predominates the density variations below 250 km altitude. Assuming a constant tidal wave input and a EUV heat input proportional to the solar activity factor $F_{10.7}$ the observed diurnal density variations and their dependence on solar activity can be quantitatively reproduced between 100 and 400 km height. The calculated density agrees with the Jacchia model (Jacchia, 1964) above 300 km and with measurements made by Priester et al. (1960), May (1963), King-Hele et al. (1965, 1967, 1968), by Taeusch et al. (1968) and by Marov (1965, 1967) below 250 km.

The time of maximum of the density variation is 14^{00} local time above 200 km. It is the natural response time of the thermosphere due to the EUV heat input. Below 200 km, where the tidal wave predominates, the time of maximum shifts toward 20^{00} at 100 km altitude.

The calculated temperature amplitudes are smaller than Jacchia's data above 200 km altitude. These differences increase with solar activity. The reason for this discrepancy is partly due to the difference in the density profiles of both models. However a relative error of about 3% must be attributed to the neglect of the diurnal variation of molecular weight in our calculations. The absolute difference between Jacchia's temperatures and ours never exceeds 6% of the total exospheric temperature.

Jacchia's (1964) empirical formula for the exospheric day and night time temperatures and their dependence on solar activity (the dashed lines in Figure 10) can be interpreted as follows: A contribution of a tidal wave from below which is independent of solar activity is superimposed on a contribution due to direct solar

EUV heat input. The amplitude of this EUV generated wave increases with solar activity and causes the increase of the exospheric temperature variation with F, while the temperature variation due to the tidal wave remains constant. The wave energy of the tidal wave is nearly completely dissipated within the thermosphere. This dissipated energy contributes to the time averaged heat input into the thermosphere. We suggest that it is responsible for the residual exospheric temperature of about 500 K at zero solar activity F 0 (see Figure 10). From Jacchia's temperature profiles one can estimate that a heat input of about 0.1 erg/cm^{2}sec above 100 km altitude is necessary to maintain an exospheric temperature of 500 K. Therefore, we estimate that the tidal wave at 100 km altitude has a wave energy of 0.1 erg/cm^{2}sec. That amount of heat energy contributes significantly to the thermospheric heat balance as can be seen by comparing it with the mean EUV heat input which varies from about 0.2 to 1 erg/cm^{2}sec between low and high solar activity.

Our two dimensional model can explain basic features of the diurnal variations within the thermosphere. However, no attempt was made to explain latitudinal variations or composition effects like the Helium bulge. Our model nevertheless describes rather well the low latitude behavior of the thermosphere which is due to the fact that the diurnal thermospheric tides are predominated by the spherical function P_{11} which is the eigenfunction of the spherical problem (Volland and Mayr, 1968b).

In Part II of this paper we shall discuss the 27 day variation, the semiannual effect and the geomagnetic activity effect.

LITERATURE

CIRA, COSPAR International Reference Atmosphere, 1965, North-Holland Publishing Company, 1965

Dalgarno, A., Ambipolar diffusion in the F-region, Journ. Atm. Terr. Phys. 26, 939, 1964

Harris, I. and W. Priester, Time dependent structure of the upper atmosphere, Journ. Atm. Sci., 19, 286-301, 1962

Jacchia, L. G., Static diffusion models of the upper atmosphere with empirical temperature profiles, Smithsonian Institution, Astrophysical Observatory, Special Report No. 170, Cambridge, Mass., 1964

Kato, S., Horizontal wind systems in the ionospheric E region deduced from the dynamo theory of the geomagnetic S_q variation. Part II: Rotating earth, Journ. Geomagn. Geoelectr. 8, 24-37, 1956

King-Hele, D. G. and J. Hingston, Variation in air density at heights near 150 km from the orbit of the satellite 1966-101J, Planet. Space Sci. 15, 1883-1893, 1967

King-Hele, D. G. and J. Hingston, Air density at heights near 190 km from the orbit of SECOR 6, Planet. Space Sci. 16, 675-691, 1968

King-Hele, D. G. and E. Quinn, Air density at heights of 150-300 km in the year 1962-1964, Planet. Space Sci. 13, 693-705, 1965

Lindzen, R. S., Thermally driven diurnal tide in the atmosphere, Quart. J. Roy. Meteorolog. Soc., 93, 18-42, 1967

May, B. R., A note on the feature and cause of the diurnal variation of neutral air density at 205 km, Planet. Space Sci., 11, 1273-1275, 1963

Marov, M. Y., Density of the upper atmosphere from the data of Soviet satellite drag, Space Research V, pp. 1140-1149, North-Holland Publishing Company, Amsterdam, 1965

Marov, M. Y., Soviet data on densities and scale heights at altitudes greater than 150 km, Space Research VIII, pp. 811-820, North-Holland Publishing Company, Amsterdam, 1968

Newton, G. P., D. T. Pelz and H. Volland, Direct, in situ measurements of wave propagation in the neutral thermosphere, Journ. Geophys. Res. 74, 1969, 183-196

Priester, W., H. A. Martin and K. Kramp, Diurnal and seasonal density variations in the upper atmosphere, Nature, 188, 202-204, 1960

Priester, W., M. Roemer and H. Volland, The physical behavior of the upper atmosphere deduced from satellite drag data, Space Sci. Rev., 6, 707-780, 1967

Taeusch, D. R., H. B. Niemann, G. R. Carignan, R. E. Smith and J. O. Ballance, Diurnal survey of the thermosphere (I) Neutral particle results, Space Research VIII, p. 930-939, North-Holland Publishing Company, Amsterdam, 1968.

Volland, H., Full wave calculations of gravity waves propagation through the thermosphere, to be published in Journ. Geophys. Res., 1969

Volland, H. and H. G. Mayr, The significance of the wave picture in the theory of diurnal tides within the thermosphere, NASA document X-621-68-166, GSFC, Greenbelt, Md., 1968a.

Volland, H. and H. G. Mayr, On the theory of the diurnal tides within the thermosphere, NASA document X-621-68-144, GSFC, Greenbelt, Md., 1968b.

Volland, H., H. G. Mayr and W. Priester, A two dimensional dynamic model of the diurnal variation of the thermosphere, Part II: An explanation of the second heat source, NASA document X-621-68-449, GSFC, Greenbelt, Md., 1968.

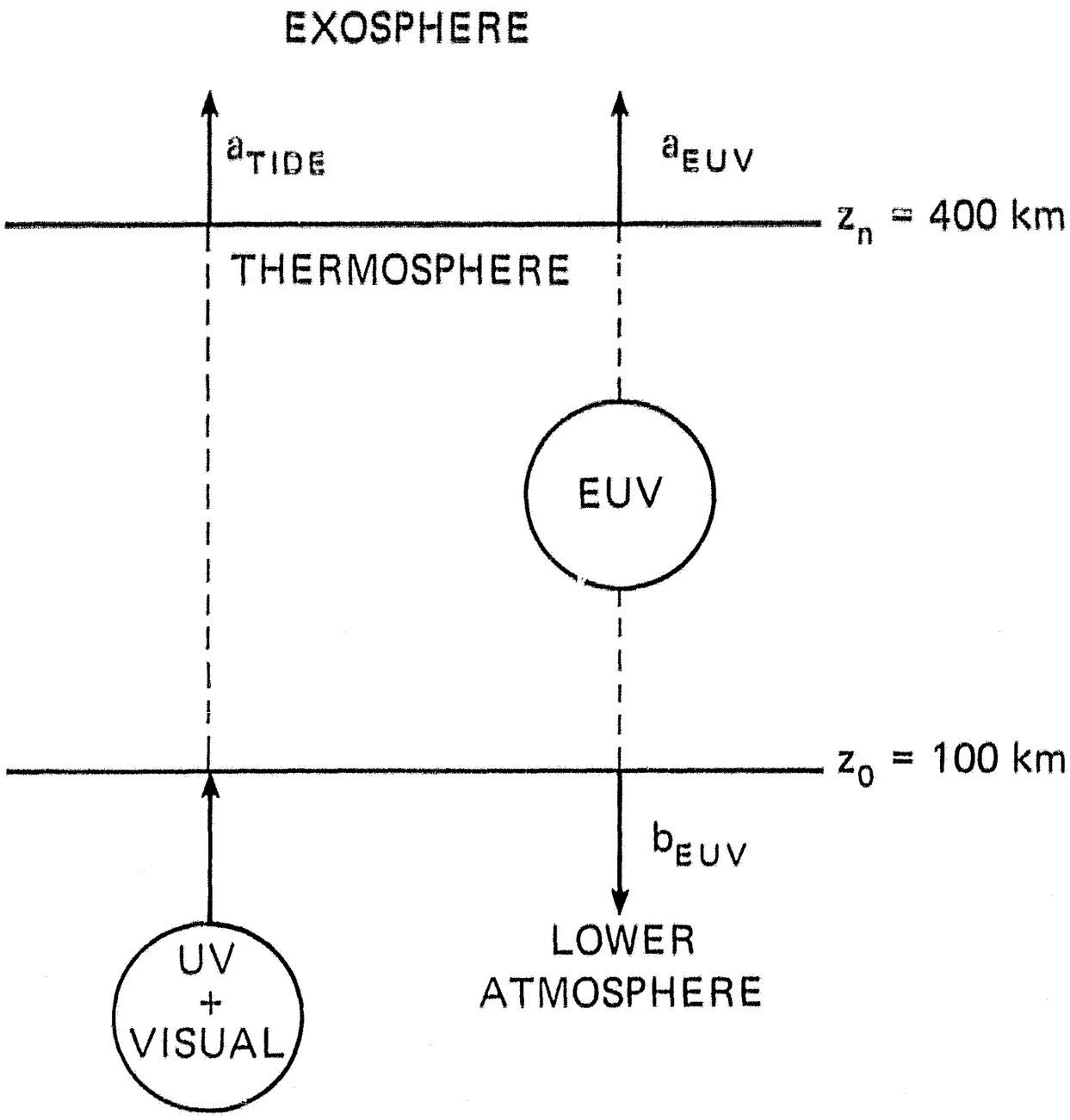

Figure 1. Block diagram showing the two energy sources which generate diurnal density disturbances within the thermosphere.

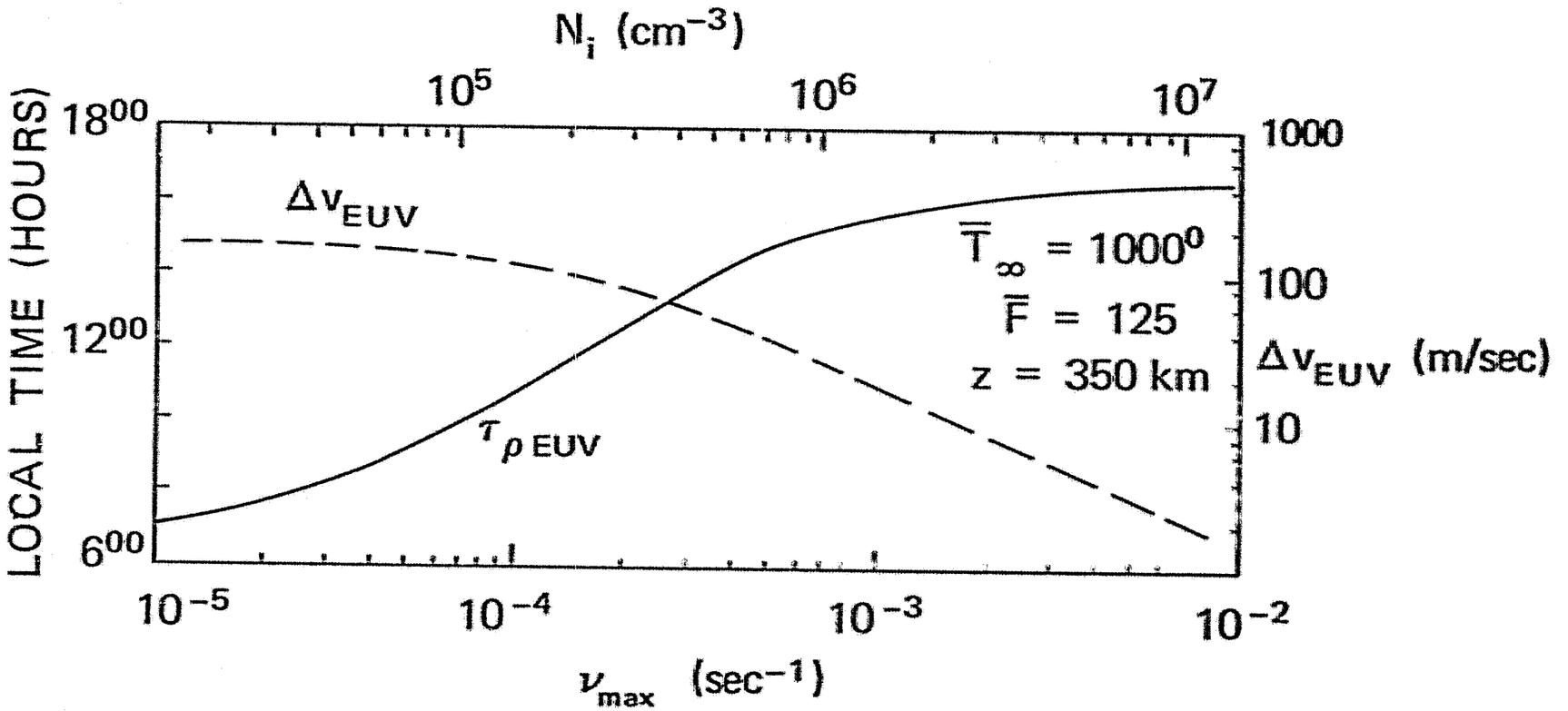

Figure 2. Time of maximum of the diurnal density variation $\tau_{\rho\,EUV}$ and the maximum horizontal wind speed Δv_{EUV} generated by solar EUV at 350 km altitude versus maximum collision number ν_{max} at the equatorial F2-layer maximum. The upper scale gives F2-maximum ion number density N_i.

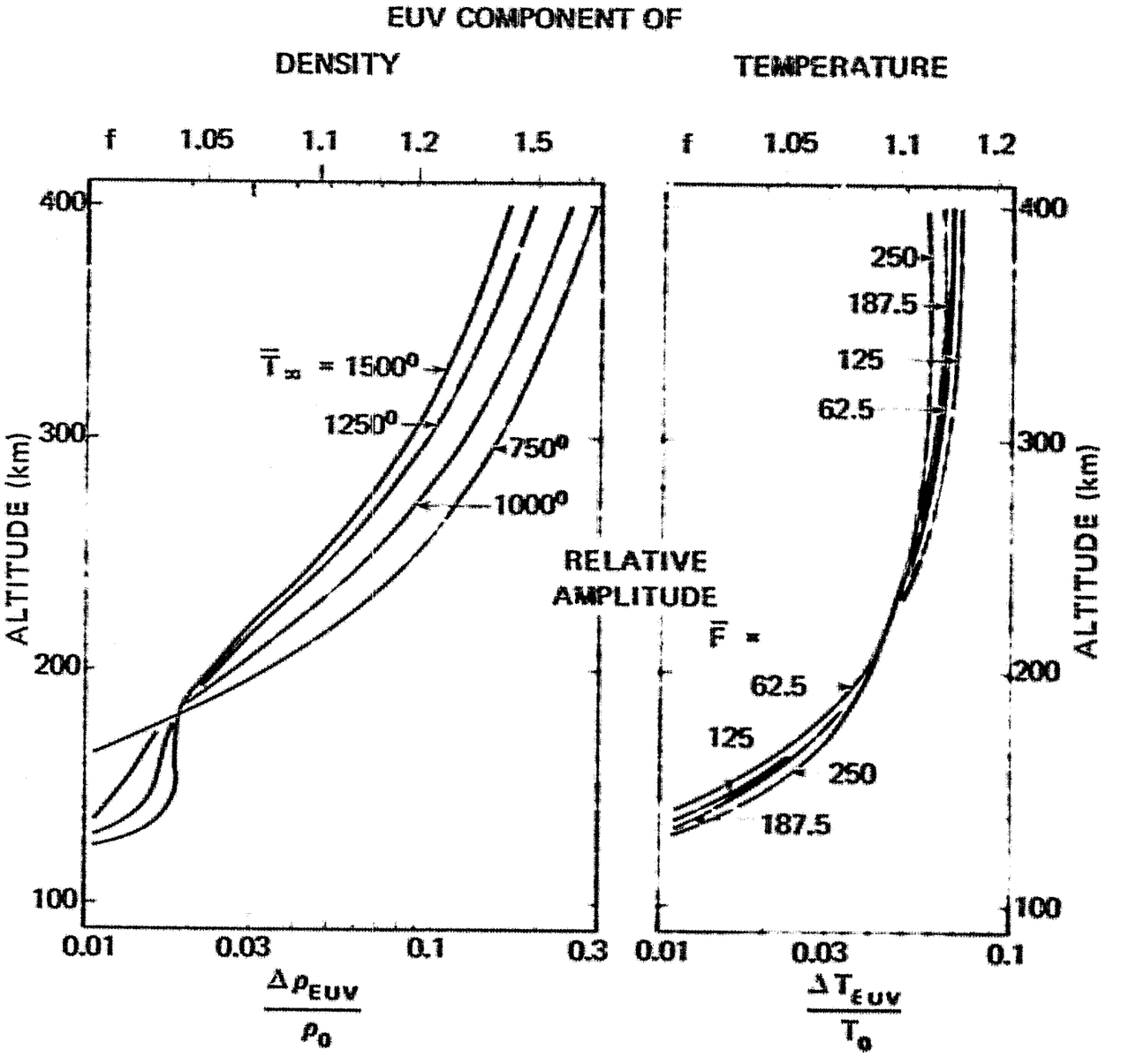

Figure 3. Diurnal density and temperature variations verses height generated by solar EUV heat input, calculated for four different thermospheric models equivalent to changing solar activity. $\bar{T}_\infty$ is the exospheric temperature of the Jacchia model (in K), $\bar{F}$ is the 10.7-cm solar flux (in 10^{-22} W/m^2 Hz). Upper scales give the ratio between maximum and minimum values f c_{max} c_{min}.

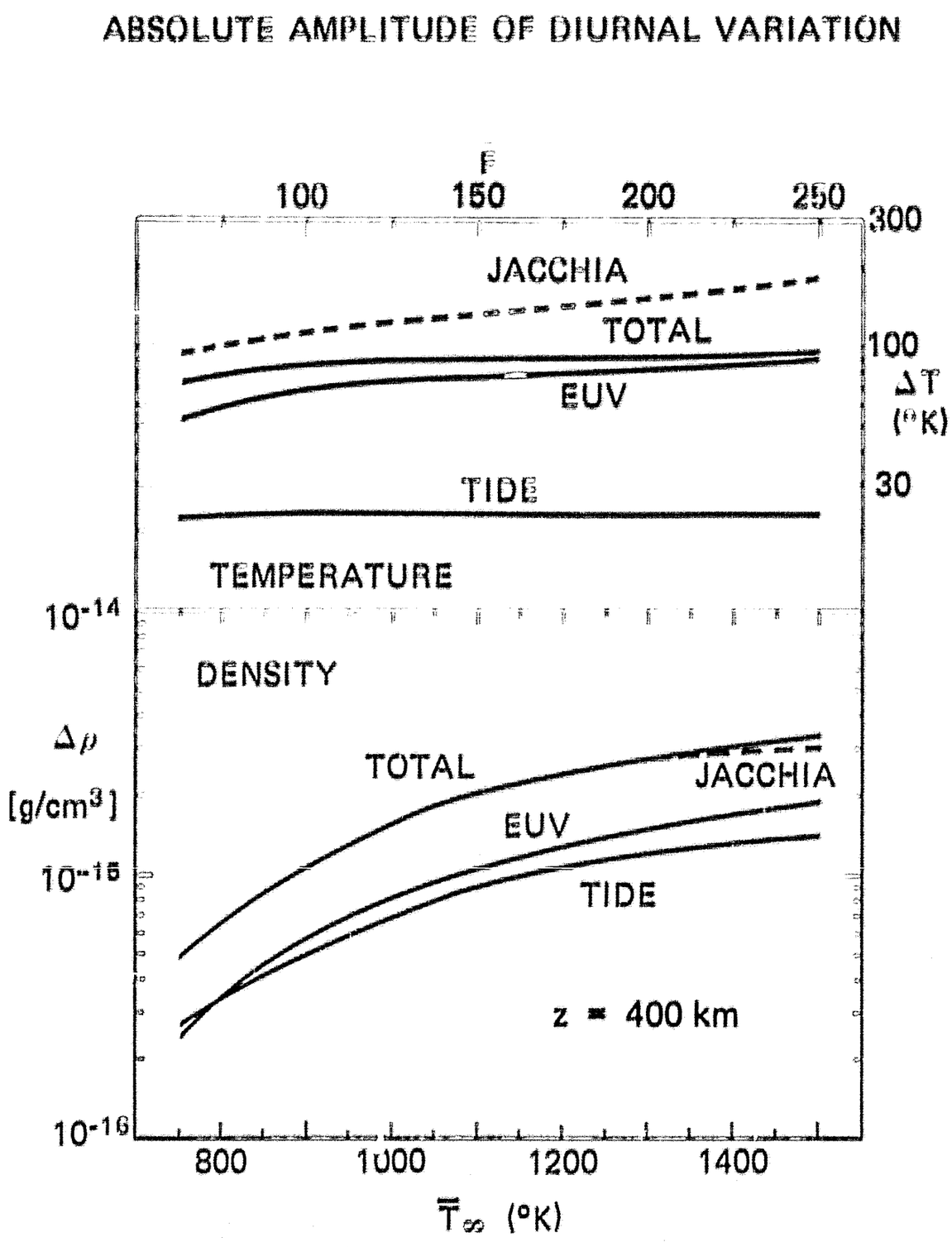

Figure 4. Absolute amplitude of diurnal density and temperature variations at 400 km altitude versus Jacchia's exospheric temperature $\bar{T}_\infty$. The dashed lines give Jacchia's model data for the difference between day and night of density and temperature at this altitude.

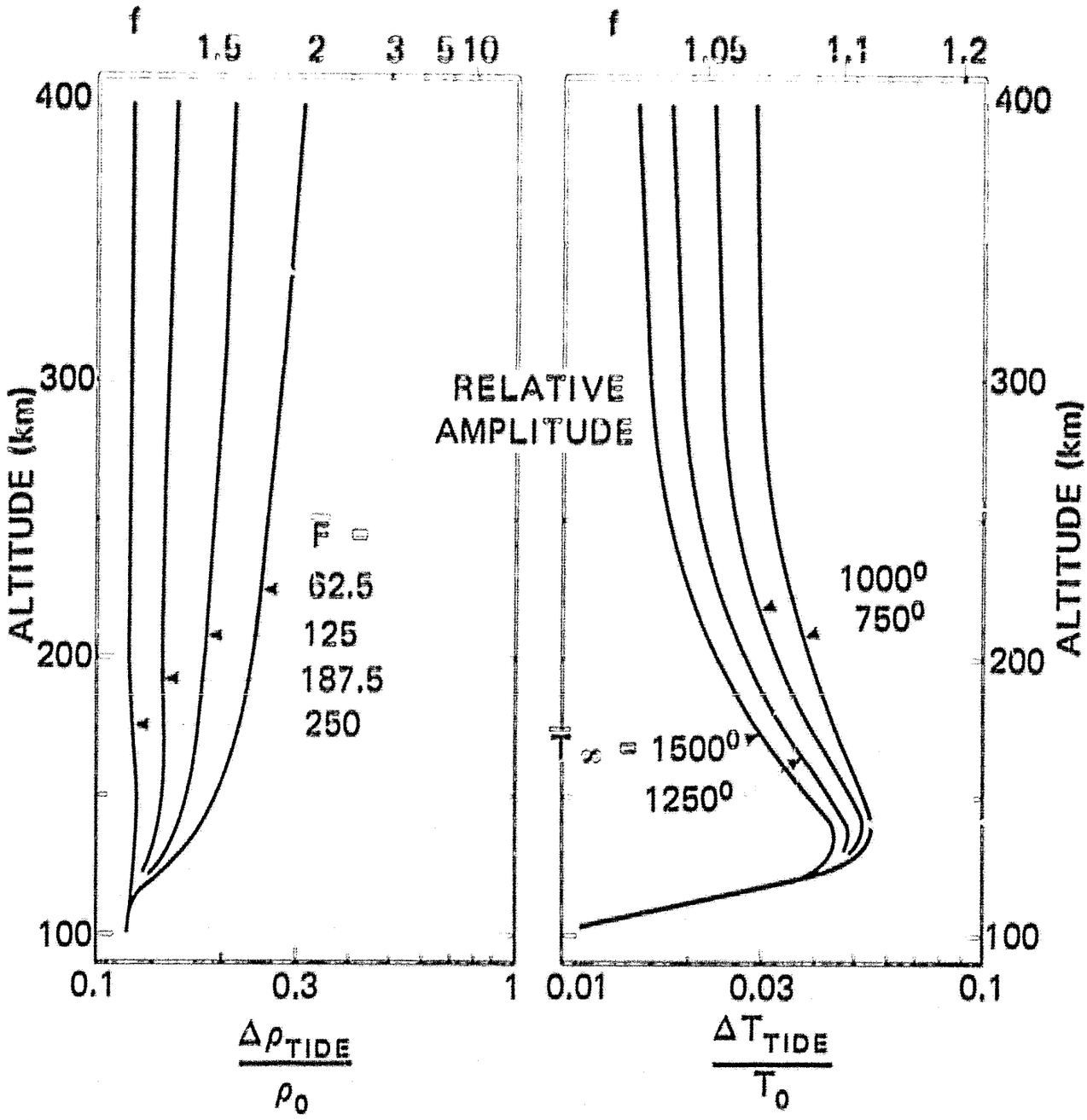

Figure 5. Diurnal density and temperature variations versus height generated by the tidal wave from the lower atmosphere, calculated for four different thermospheric models equivalent to changing solar activity. $\bar{T}_\infty$ is the exospheric temperature of the Jacchia model (in °K), $\bar{F}$ is the 10.7-cm solar flux (in 10^{-22} W m^2 Hz). Upper scales give the ratio between maximum and minimum values f c_{max} c_{min}.

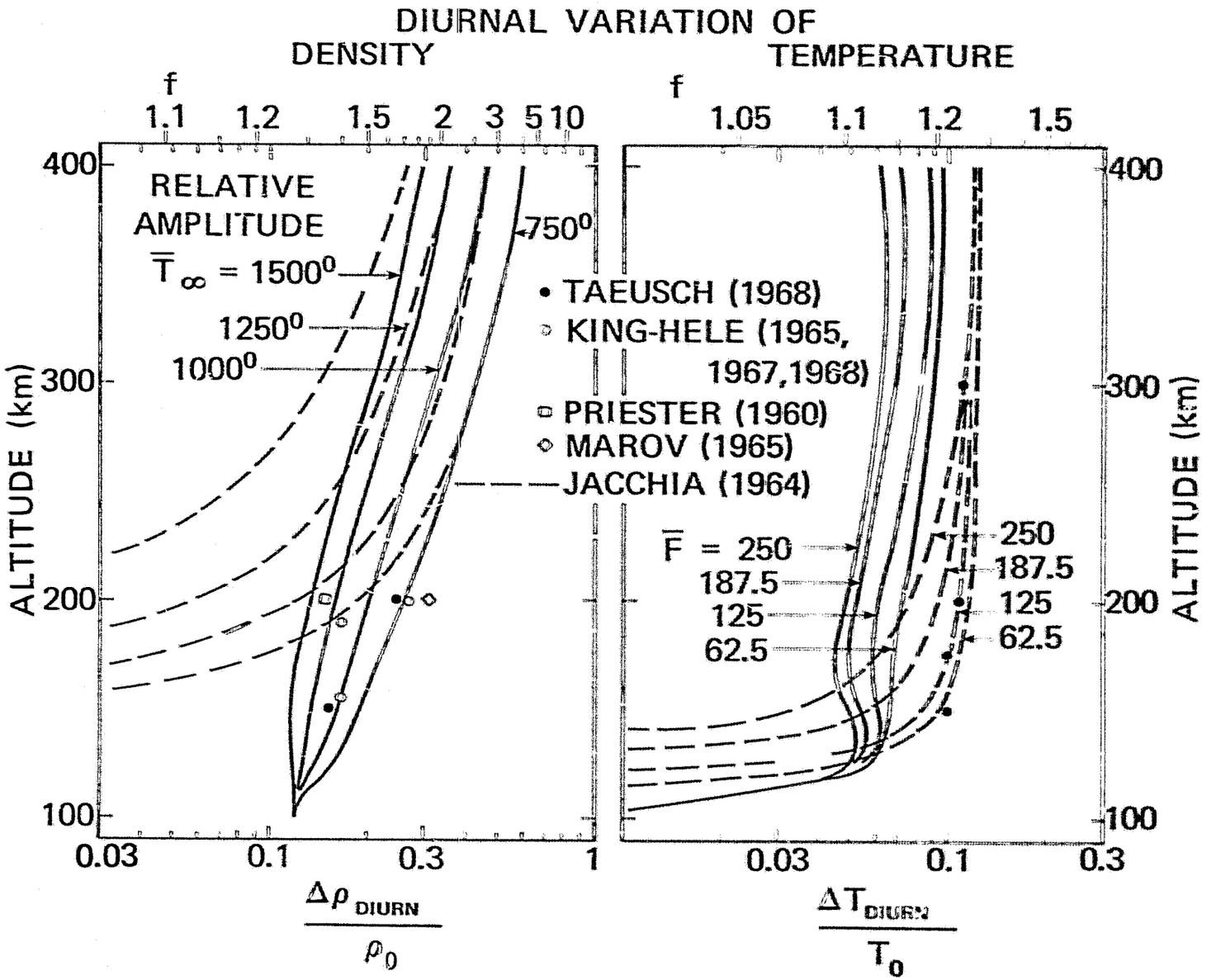

Figure 6. Total diurnal density and temperature variations versus height generated by solar EUV and by the tidal wave, calculated for four different thermospheric models equivalent to changing solar activity. $\bar{T}_\infty$ is the exospheric temperature of the Jacchia model (in °K), $\bar{F}$ is the 10.7-cm solar flux (in 10^{-22} W/m^2 Hz). Upper scales give the ratio between maximum and minimum values $f = c_{max}\ c_{min}$.

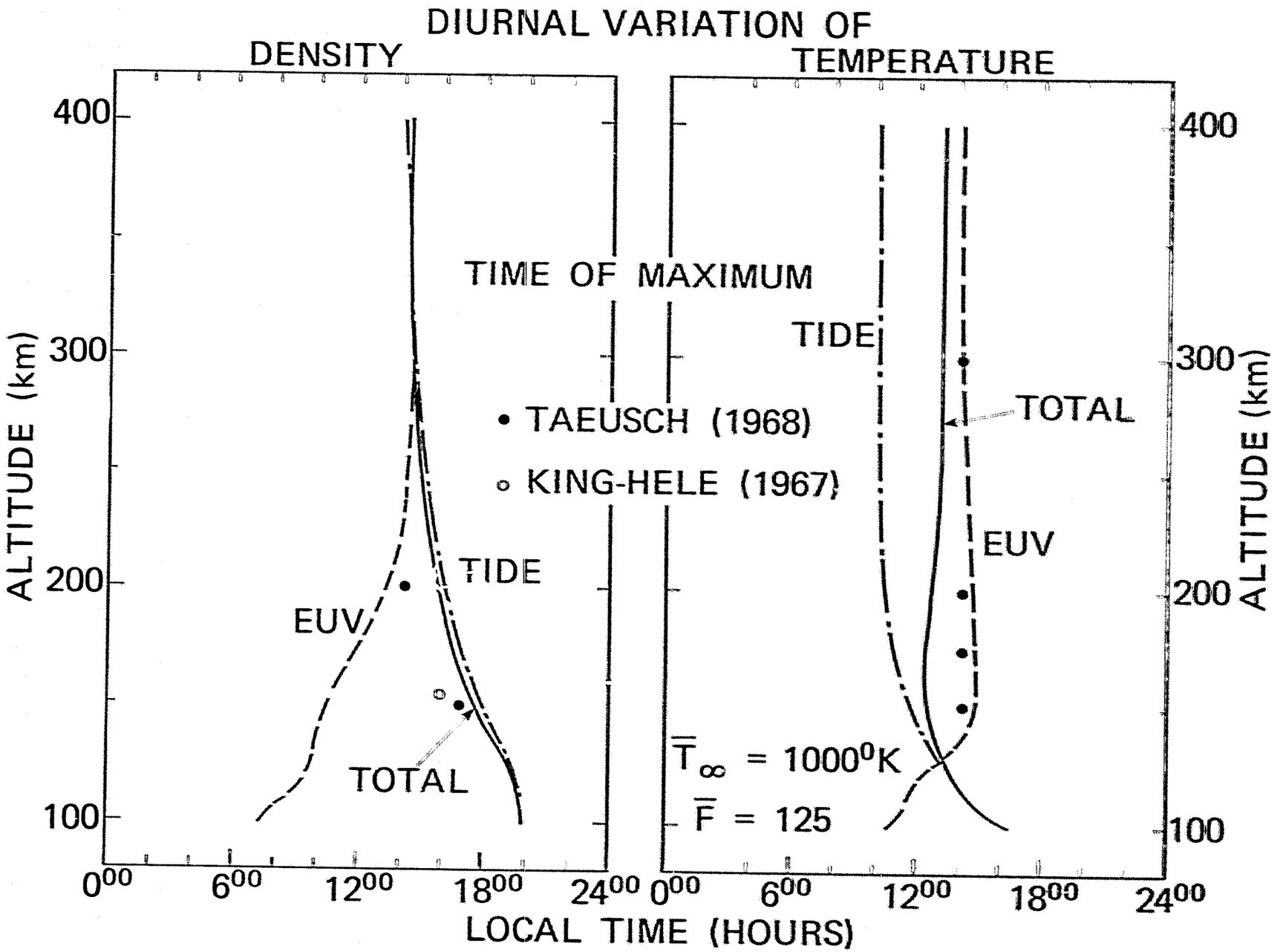

Figure 7. Time of maximum of the diurnal variations of density and temperature versus height, calculated for a thermospheric model of exospheric temperature of $\overline{T}_\infty$ = 1000°K.

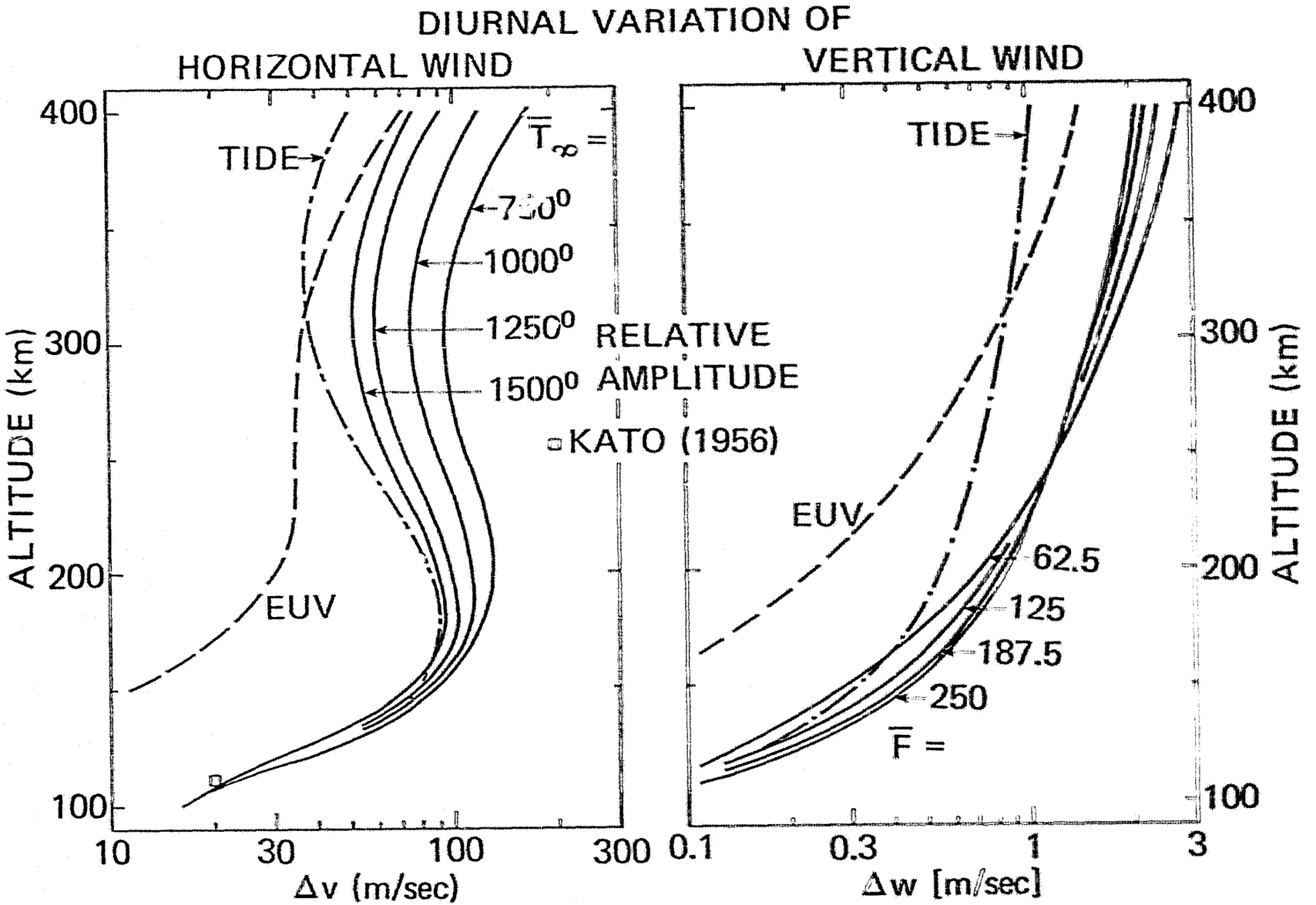

Figure 8. Diurnal variation of horizontal and vertical winds versus height calculated for four different thermospheric models equivalent to changing solar activity. $\bar{T}_\infty$ is the exospheric temperature of the Jacchia model (in K), $\bar{F}$ is the 10.7-cm solar flux (in 10^{-22} W/m^2 Hz). Dashed and dash-dotted lines give the contributions of EUV and of the tidal wave, respectively, calculated for $\bar{T}_\infty$ = 1000°K.

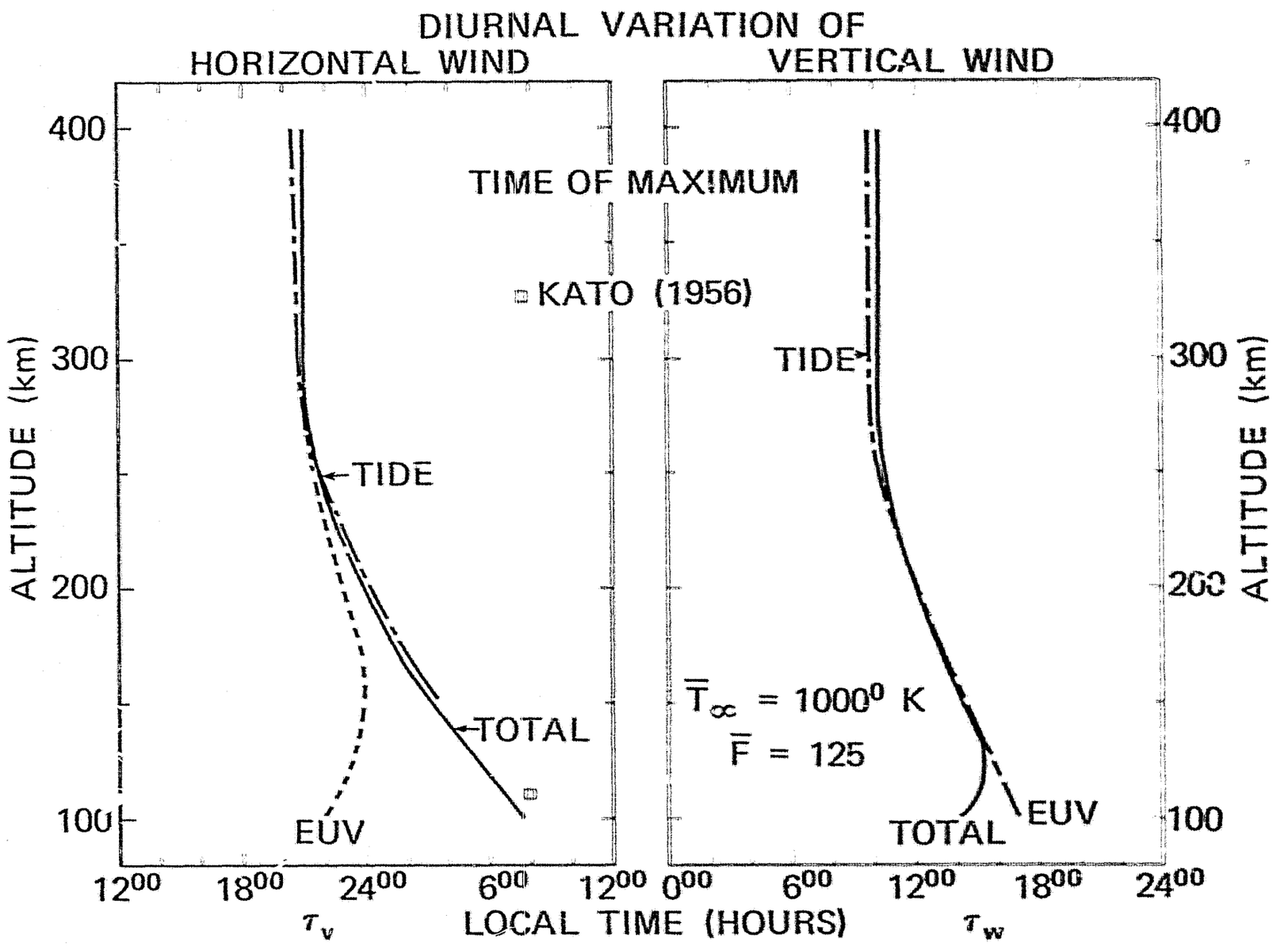

Figure 9. Time of maximum of the diurnal variations of horizontal and vertical winds, calculated for a thermospheric model of exospheric temperature of $\bar{T}_\infty$ = 1000 K.

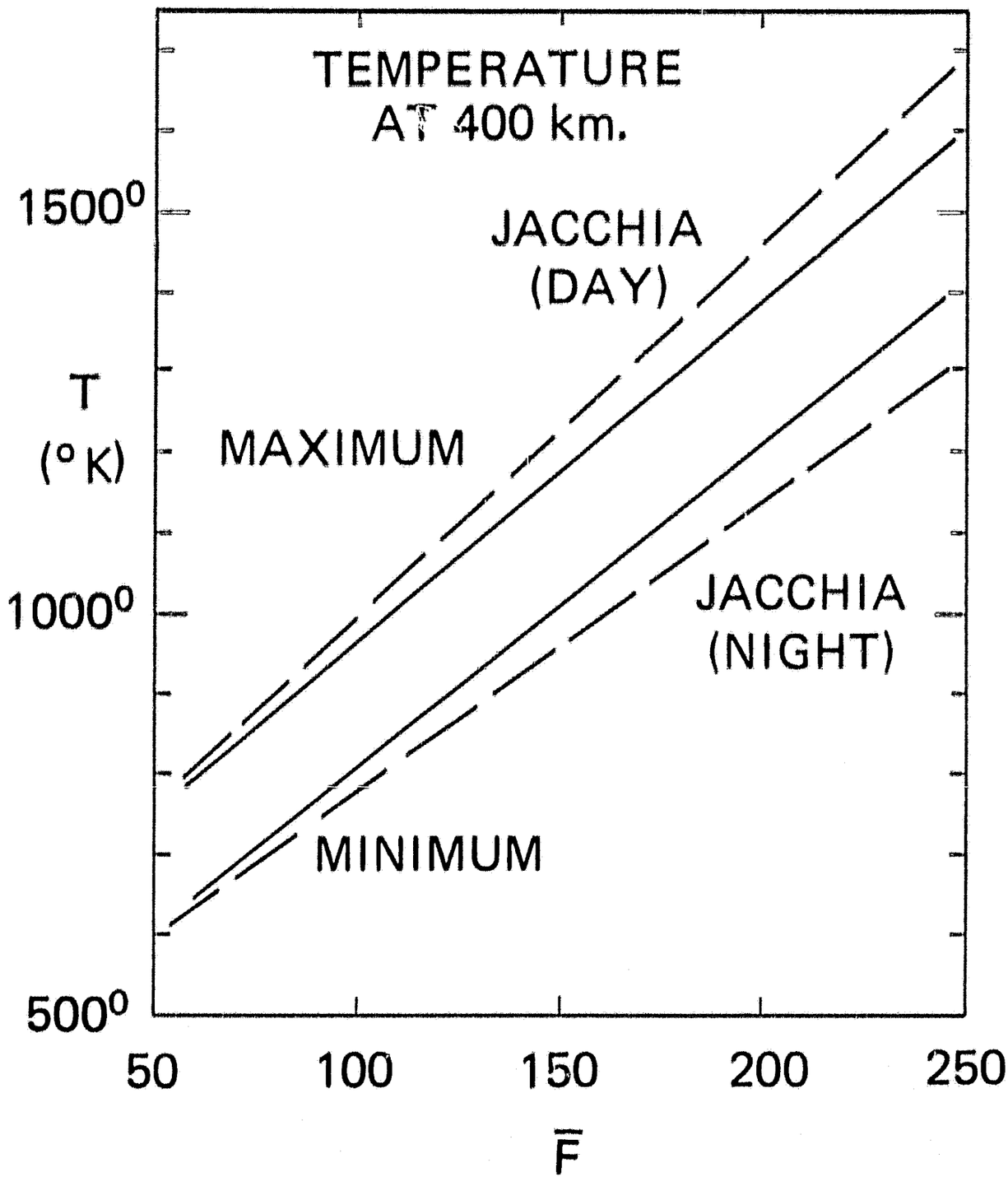

Figure 10. Calculated maximum and minimum temperatures at 400 km altitude versus solar activity factor $\bar{F}$. The dashed lines give the exospheric temperatures of the Jacchia model at day and at night.